

## SUPPORTING INFORMATION

### **Determination of Schottky barrier height and enhanced photoelectron generation in novel plasmonic immobilized multisegmented (Au/TiO<sub>2</sub>) nanorod arrays (NRAs) suitable for solar energy conversion applications**

Muhammad Shahid Arshad<sup>a,\*</sup>, Špela Trafela<sup>b</sup>, Kristina Žužek Rožman<sup>b</sup>, Janez Kovač<sup>c</sup>, Petar Djinović<sup>a</sup> and Albin Pintar<sup>a</sup>

<sup>a</sup>Department for Environmental Sciences and Engineering, National Institute of Chemistry, Hajdrihova 19, SI-1001 Ljubljana, Slovenia

<sup>b</sup>Department for Nanostructured Materials, Jožef Stefan Institute, Jamova 39, SI-1000 Ljubljana, Slovenia

<sup>c</sup>Department of Surface Engineering and Optoelectronics, Jožef Stefan Institute, Jamova 39, SI-1000 Ljubljana, Slovenia

\*Email - shahid.arshad85@gmail.com, shahid.arshad@ki.si

## 1. Discrete dipole approximation (DDA) simulations

The interaction of the electromagnetic radiation with Au and multisegmented Au/TiO<sub>2</sub> NRs were simulated using nanoDDSCAT+ software <sup>1</sup>. This code is based on discrete dipole approximation (DDA) method originally developed by Purcell and Pennypacker <sup>2</sup> and improved by Draine et al. <sup>3</sup>. The utilized numerical method divides any arbitrary shaped object into a finite, cubic array of polarizable points (dipoles) and the electric field radiated by the object is calculated by solving Maxwell equations by taking into account interactions between all dipoles. For the accuracy of calculations, large number of dipoles  $N$  should be taken into consideration to (1) reproduce satisfactorily the target geometry and also (2) diminish the inaccuracy originating from the surface granularity. The optimum number  $N$  is somewhat arbitrarily taken as a number for which the numerical results converge to a certain value and change little by further increases in  $N$ . The approach utilized in our simulations and the accuracy of the code was successfully tested by closely reproducing the already published results <sup>4,5</sup>. All nanoDDSCAT+ simulations were run on online tool (nanoHUB.org) <sup>1</sup>.

The local electric field enhancement ( $|E|^2/|E_0|^2$ ) across the surface of the Au/TiO<sub>2</sub> NRs was obtained from incident field amplitude  $|E_0|$  and macroscopic field amplitude  $|E|$  at each grid point of a volume surrounding the nanostructure. For the modelling of optical properties of Au NRs, cylinders with flat ends were considered. The dielectric function of Au was taken from Johnson and Christy <sup>6</sup>, the dielectric function for amorphous TiO<sub>2</sub> is similar to anatase<sup>7</sup> was taken as constant ( $\epsilon=2.488$ ) from <sup>8</sup>.

### 1.1. Longitudinal modes of Au NRs in air

Y-polarized light was used with electric field oscillating such that in all cases L-mode was excited

along the long axis of Au NRs. The refractive index of surrounding media was set to air. Fig. S1a is showing the extinction spectra of Au NRs with fixed diameter at 40 nm and the length was changed, resulting in aspect ratio (AR) = 1.7, 2.57, 3.75, 4.28, 5, and 6.28. Upon increasing the AR of Au NRs, the values of the L-mode maxima are centered at 554, 648, 770, 830, 910 and 1030 nm, respectively, as shown in Fig. S1a. The peak broadening was observed with increasing the AR of Au NRs. Such phenomenon is associated with the increasing scattering efficiency when increasing the size of Au NRs due to the damping mechanism involved<sup>9</sup>. It is clearly seen that maximum extinction efficiency ( $\lambda_{max}$ ) has been red shifted with increasing AR of Au NRs. Hence, AR is a key parameter determining the optical properties of Au NRs. Furthermore, Fig. S1b shows  $\lambda_{max}$  as a linear function of AR for Au NRs in the given range of dimensions. The simulated data was fitted to obtain the following linear equation:

$$\lambda_{max} = 96AR + 418 \quad (1)$$

Such equations are desirable as they allow predicting  $\lambda_{max}$  for Au NRs; the only required information is their AR. Thus, the  $\lambda_{max}$  changes significantly with the AR of Au NRs.

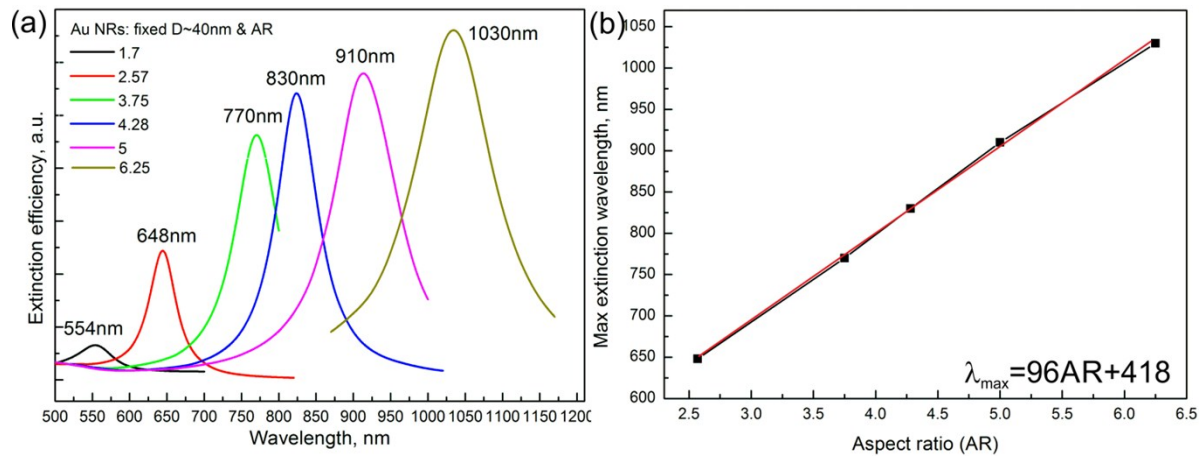


**Fig. S1.** (a) The extinction spectra of Au NRs with various AR. (b) Linear relationship between  $\lambda_{\max}$  and AR for Au NRs.

## 1.2. Optical properties of multisegmented (Au/TiO<sub>2</sub>) NRs in air

In multisegmented (Au/TiO<sub>2</sub>) NRs, the TiO<sub>2</sub> and Au segments were defined by dielectric functions which were obtained from <sup>8</sup> and <sup>6</sup>, respectively. The corresponding  $\lambda_{\max}$  values of the L-mode for Au control and Au/TiO<sub>2</sub> NRs appear at 770 and 690 nm, respectively, as shown in Fig. S2. The observed blue shift for Au/TiO<sub>2</sub> is due to the introduction of the TiO<sub>2</sub> segment. In detail, the incident electric field induces both the free electron oscillation in the Au segment and the strong polarization charge oscillation in TiO<sub>2</sub> segment because of its high refractive index. The charges in both segments can interact through Coulombic force. Such an interaction leads to constructive or destructive interference between the free electron and polarized charge oscillations. The destructive interference reduces the total oscillation strength of plasmonic metal due to the partial cancellation from polarization charge oscillations; as a result, amplitude of L-mode significantly reduced as shown in Fig. S2.

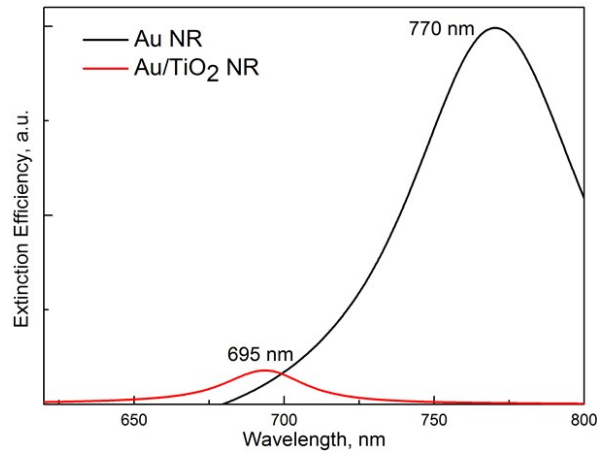


**Fig. S2.** The extinction spectra of Au and multisegmented Au/TiO<sub>2</sub> NR with the same AR.

## 2. Free standing hexagonally arranged arrays of Au NRs

The  $\lambda_{\max}$  of L-mode is very sensitive to characteristics of the particle arrangements and the single particle behavior significantly modified by interactions between the particles. Here we discuss the long range plasmon interactions in the gaps between hexagonally arranged Au NRs because of their strong dipole-dipole interactions through NFE, which can be as high as  $|E|^2 \sim 10^4$  <sup>10</sup>.

Fig. S3a is showing the schematic of 7 hexagonally arranged NRs with the diameter (D) of  $\sim 7.5$  nm and length of  $\sim 25$  nm (AR $\sim 3.33$ ). For isolated single Au NR (blue line) the calculated  $\lambda_{\max}$  of L-mode is around 650 nm (Fig. S4b). The corresponding  $\lambda_{\max}$  values of the L-mode for 7 Au NRs separated by S=15 and 20 nm appears at 575 and 610 nm, respectively. It is clearly seen that  $\lambda_{\max}$  of L-mode is blue shifted as a function of the separation between the NRs. It is evident from Fig. S3b that the intensity of the L-mode decreased as separation between the Au NRs is reduced. This indicates that it is hard to excite hexagonally arranged Au NRs when they are very closely aligned with each other. The observed behavior of the L-mode can be explained by the formation of a spatially extended collective plasmonic resonance in the array caused by the interaction between the L-modes supported by the Au NRs. Such interactions result in the formation of the band of

plasmonic states of the NRs assembly as can be clearly seen at 700 and 680 nm for  $S=15$  nm (red line) and 20 nm (black line) as shown in Fig. S3b, respectively.

The electric field enhancement associated with the L-mode (top view) of the Au NR array with the separation of 15 and 20 nm is shown in Fig. S3c and S3d, respectively. For the larger inter-rod distance of 20 nm, the field is localized at the NRs extremities as expected for the L-mode and didn't couple strongly with neighboring rods as shown in Fig. S3d. However, the effect of a reduction in the inter-rod distance (e.g.  $S=15$ ) leads to a strong coupling of the L-mode as shown in Fig. S3c. Thus, it is clear that the strong coupling of the electric field is accountable for the blue shift in  $\lambda_{\max}$  as shown in Fig. S3b.

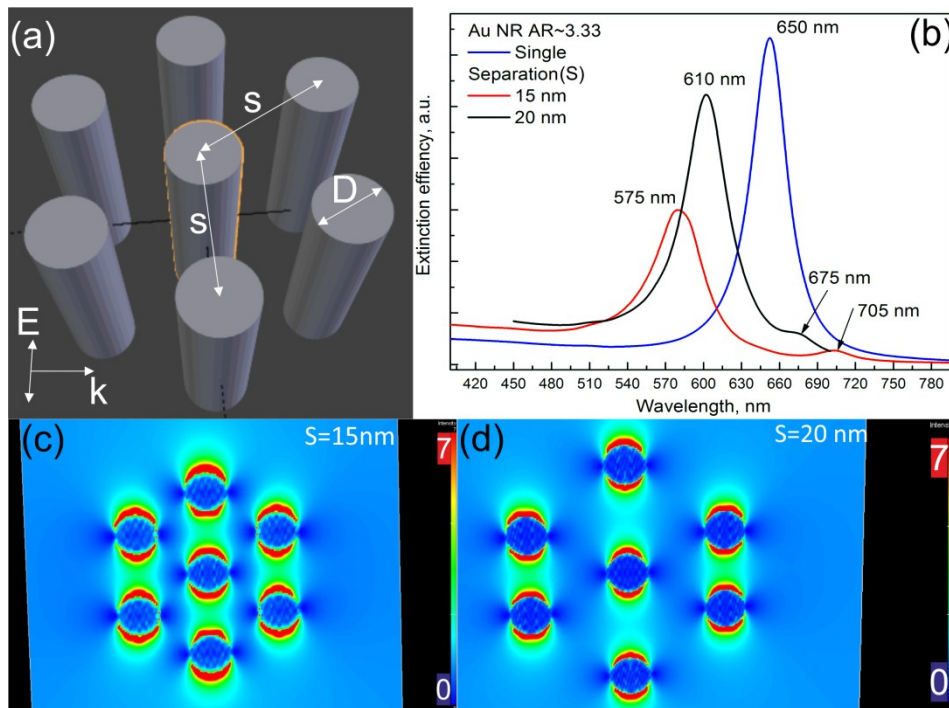


**Fig. S3.** (a) Hexagonally arranged 7 NRs separated by distance ( $S$ ) with diameter ( $D$ ). (b) Extinction spectra of a single isolated Au NR and Au NRs in arrays with different separations ( $S=15$  and 20 nm). The electric field enhancement of hexagonally arranged Au NRs with the separation of around (c) 15 nm and (d) 20 nm.

## XPS data on TiO<sub>2</sub> and Au/TiO<sub>2</sub> NRAs

XPS survey spectra of TiO<sub>2</sub> (black curve) and Au/TiO<sub>2</sub> (red curve) NRAs is shown in Fig. S4.

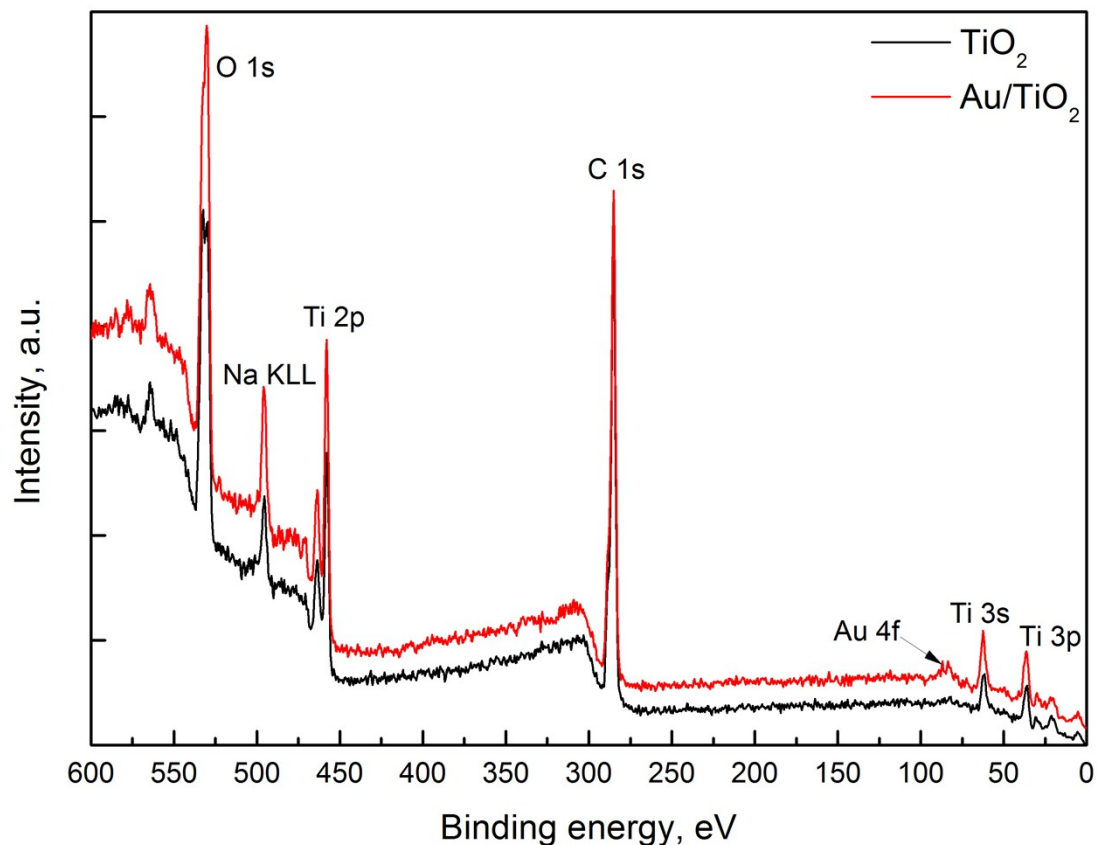


**Fig. S4.** XPS survey spectrum of pure TiO<sub>2</sub> and Au/TiO<sub>2</sub> NRAs.

## References

1. A. N. Sobh , S. White , J. Smith , N. Sobh and P. K. Jain nanoDDSCAT+, <https://nanohub.org/resources/21414>, (accessed April, 2016).
2. E. M. Purcell and C. R. Pennypacker, *Astrophys. J*, 1973, **186**, 705-714.
3. B. T. Draine and P. J. Flatau, *J. Opt. Soc. Am. A*, 1994, **11**, 1491-1499.
4. A. Brioude, X. C. Jiang and M. P. Pileni, *J. Phys. Chem. B*, 2005, **109**, 13138-13142.
5. S. W. Prescott and P. Mulvaney, *J. Appl. Phys.*, 2006, **99**, 123504.

6. P. B. Johnson and R. W. Christy, *Ph. Rv. B*, 1972, **6**, 4370-4379.
7. B. Prasai, B. Cai, M. K. Underwood, J. P. Lewis and D. A. Drabold, *JMatS*, 2012, **47**, 7515-7521.
8. K. Awazu, M. Fujimaki, C. Rockstuhl, J. Tominaga, H. Murakami, Y. Ohki, N. Yoshida and T. Watanabe, *J. Am. Chem. Soc.*, 2008, **130**, 1676-1680.
9. K.-S. Lee and M. A. El-Sayed, *J. Phys. Chem. B*, 2005, **109**, 20331-20338.
10. MerleinJorg, M. Kahl, A. Zuschlag, A. Sell, A. Halm, J. Boneberg, P. Leiderer, A. Leitenstorfer and R. Bratschitsch, *Nat Photon*, 2008, **2**, 230-233.